https://doi.org/10.5194/egusphere-2025-1700
Preprint. Discussion started: 9 May 2025

Chemical characterization and source apportionment of fine particulate matter in Eastern Africa using aerosol mass spectrometry.

Theobard Habineza[1], Allen L. Robinson[2], H. Langley DeWitt[3], Jimmy Gasore[4], Philip L. Croteau[5], Albert A. Presto[*1,4]

[1]Carnegie Mellon University, Department of Mechanical Engineering and Center for Atmospheric Particle Studies (CAPS)

[2]Department of Atmospheric Science, Colorado State University

[3]CIRES, University of Colorado, Boulder, CO, USA

[4] Kigali Collaborative Research Center, Kigali, Rwanda

[5]Aerodyne Research, Inc., Billerica, Massachusetts, USA

*Corresponding author: apresto@andrew.cmu.edu

Abstract.

Ambient air pollution poses a significant threat to public health, particularly in low and middle-income countries, where detailed data on particulate matter (PM) mass and composition are scarce. We conducted a year-long study on PM composition and sources in Eastern Africa (Kigali, Rwanda). The annual mean concentration of PM_1 was 31 µg/m³, with slightly higher concentrations during the dry season. Organic aerosols (OA) contributed 73% of the observed PM_1 mass, black carbon (BC) 16%, nitrate 6%, sulfate and ammonium 2% each, and chlorine 1%. BC is approximately 60% due to fossil fuel and 40% from biomass burning emissions. Tracer ions detected by the mass spectrometer suggest that photochemistry plays a significant role in the formation of secondary OA during the daytime (6:00 am to 6:00 pm), while primary OA dominates in the morning and evening due to increased anthropogenic activity and shallower boundary layer height. PM_1 in Kigali is primarily composed of Oxygenated Organic Aerosols (OOA, 45%), Hydrocarbon-like OA (HOA, 32%), and Biomass Burning OA (BBOA, 23%). Secondary organic aerosol (SOA) accounted for 47% and 41% of PM_1 during the wet and dry seasons, respectively, while primary OA (POA: BBOA + HOA) contributed 53% and 59%. This suggests that seasonal changes in

https://doi.org/10.5194/egusphere-2025-1700
Preprint. Discussion started: 9 May 2025

PM_1 mass in Kigali are primarily driven by deposition rather than shifts in emissions, chemical processing, or source strengths.

1. Introduction

Air pollution exposure has severe impacts on public health. Air pollution is classified as the second leading risk factor for deaths in Africa(Health Effects Institute. 2022). The adverse effects of air pollution manifest as cardiovascular diseases, respiratory diseases, and cerebrovascular diseases(Brito et al. 2018a; Health Effects Institute. 2022; WHO 2025, n.d.). In 2019, ambient air pollution was estimated to cause 4.2 million premature deaths globally, with 89% occurring in low- and middle-income countries (LMICs), including 1.1 million deaths in Africa. (UN Environment 2019; WHO 2025, n.d.) Studies in the Global South, including Eastern Africa, have revealed that particulate matter (PM), defined as solid or liquid particles suspended in the air, is the air pollutant most responsible for human health impacts and a leading risk factor across sub-Saharan Africa (SSA)(Health Effects Institute 2022). PM mass concentrations in Africa often reach unhealthy levels compared to the World Health Organization's (WHO) air quality guidelines, posing significant health risks to public health and the environment (Gaita et al. 2014a; Langley Dewitt et al. 2019; Onyango et al. 2024a; Singh et al. 2021a, 2021b). Rapid population growth, urbanization, energy consumption, and motorization have been reported as drivers of air pollution in LMICs (Abera et al. 2021; Brito et al. 2018b; Health Effects Institute. 2022; REMA 2018a).

Eastern Africa and the Global South, in general, face a noticeable scarcity of air pollution measurements(AirNow 2025; openaq 2025). This hinders the understanding of air pollution impacts. Developing effective regulatory strategies requires information on air pollutant sources, which in turn require measurements of PM composition. The data gaps are even larger for PM composition measurements than for PM mass concentrations(Dhammapala 2019).

The few published studies on air pollution in Eastern Africa showed that PM concentrations exceed the WHO guidelines(Gahungu and Kubwimana 2022a; Kalisa, Kuuire, and Adams 2023; McFarlane et al. 2021; Ndamuzi et al. 2024a; Onyango et al. 2024a; REMA 2018a) and higher concentrations of $PM_{2.5}$ (particulate matter smaller than 2.5 microns in diameter) are present in urban areas(Health Effects Institute. 2022). $PM_{2.5}$ concentrations in eastern African cities are 3 to >10 times higher than the 5 $\mu g/m^3$

https://doi.org/10.5194/egusphere-2025-1700
Preprint. Discussion started: 9 May 2025

air quality guidelines (AQG) set forth by the World Health Organization. Gahungu and Kubwimana(Gahungu and Kubwimana 2022b) used low-cost sensors and found that the daily mean concentration of $PM_{2.5}$ in Kigali, Rwanda, was approximately 30 µg/m³ in the rainy season and 55 µg/m³ in the dry season. Kalisa et al. measured hourly average $PM_{2.5}$ concentrations of 25 µg/m³ in the city center of Kigali(Kalisa et al. 2018). Onyango et al., using US State Department $PM_{2.5}$ monitor data and filter collection, reported that the mean $PM_{2.5}$ in Kampala, Uganda is 59.4 µg/m^3 (Onyango et al. 2024a). McFarland et al. reported mean $PM_{2.5}$ concentrations of 43.5 µg/m^3 in the central African city of Kinshasa, Democratic Republic of Congo (DRC). (McFarlane et al. 2021). Ndamuzi et al., using low-cost sensors coupled with mathematical models, reported an annual mean $PM_{2.5}$ of 35.0 µg/m³ in Bujumbura, Burundi (Ndamuzi et al. 2024a).

There is limited information on PM composition and sources in Eastern Africa. Studies on $PM_{2.5}$ chemical speciation and source apportionment in Eastern Africa identified traffic emissions (36%) and biomass/secondary aerosols (28%) as the main sources of $PM_{2.5}$ in Mbarara, Uganda(Onyango et al. 2024b)while mineral dust and traffic emissions together account for 74% of $PM_{2.5}$ in Nairobi, Kenya(Gaita et al. 2014b). The chemical composition and sources of $PM_{2.5}$ in other Eastern African cities are still unexplored, and without detailed data on PM composition, source identification remains unknown.

Rwanda, an Eastern African country, is experiencing rapid population growth in its urban centers, particularly in its capital city, Kigali. The annual rate of urbanization is 4.1%, contributing to a high population density of 2,330 inhabitants per km^2 as of 2023(Kigali city 2024b). Notably, 85% of households in Kigali rely on biomass burning for cooking, which includes wood, charcoal, and waste materials(MINEFRA 2018a). Additionally, 13% of households use petroleum-based fuels such as diesel, kerosene, and liquified petroleum gas (LPG), while 2% utilize electricity for cooking(MINEFRA 2018a; Rwanda Ministry of infrastructure 2018). In 2019, air pollution-related deaths in Rwanda were estimated at 9,286, and an estimated economic cost of $349 million(Fisher et al. 2021), following a rise of 41% from 2008 to 2019 (GBD 2024; Taghian et al. 2024).

To better understand PM chemical composition, concentration, and sources in Eastern Africa, we conducted long-term ground measurements of PM mass concentration and chemical composition using

https://doi.org/10.5194/egusphere-2025-1700
Preprint. Discussion started: 9 May 2025

an aerosol mass spectrometer at a central site in Kigali, Rwanda. This study uses a 12-month(April 2023 to May 2024) dataset that captures the four alternating rainy and dry seasons in Rwanda and Eastern Africa in general. These data represent the first mass spectrometry-based PM composition measurements in the region, offering high-time resolution insights. The findings not only enhance an understanding of PM composition but also provide a vital tool for policymakers to develop data-driven air pollution mitigation strategies and targeted interventions in this region.

2. Methods

2.1 Sampling location

Real-time PM_1 data were collected from April 2023 to May 2024 at a fixed monitoring station located at the University of Rwanda, College of Science and Technology (UR/CST) at latitude -1.9619, longitude 30.0645 in Nyarugenge District, Kigali City (Figure S1, Supporting Information).

Kigali is characterized by rolling hills, with steep slopes connecting a network of valleys and ridges at an altitude of approximately 1,500 meters above sea level(Rwanda Meteo 2025). The monitoring site is in the city center, on the third floor of a three-story building at UR/CST. The site is surrounded by a mix of commercial and residential neighborhoods, with busy roads in the city center in Nyarugenge District, making it representative of an urban background station.

Like many Eastern African cities, Kigali experiences four alternating seasons: the long dry season (June, July, and August), the short rainy season (September, October, and November), the short dry season (December, January, and February), and the long rainy season (March, April, and May). The annual average rainfall in Kigali is 1170 mm, the annual mean temperature is 22^{o} C, and the annual maximum temperature is 33^{0} C(Kigali city 2024b; World bank 2021).

Kigali City is experiencing rapid urbanization with a population of 1,745,555 inhabitants(Kigali City 2024a), leading to an increase in traffic and frequent traffic congestion. As of 2018, the vehicle fleet in Kigali was dominated by imported used vehicles, with 95.2% of the total fleet being older than 10 years. (UN Environment 2018; UN Environment 2019) These vehicles burn high-sulfur fuel, as the fuels used in most eastern African countries are 50 ppm sulfur for diesel and 100 ppm sulfur for gasoline(Environmental Compliance institute 2018; Miller and Jin 2018).

https://doi.org/10.5194/egusphere-2025-1700
Preprint. Discussion started: 9 May 2025

2.2 In-situ measurements of PM and BC

A quadrupole Aerosol Chemical Speciation Monitor (Q-ACSM) from Aerodyne Research was used to measure the ambient concentration and composition of non-refractory PM_1 (NR-PM_1) in real-time (Ng, Herndon, et al. 2011a). The ACSM uses aerosol mass spectrometry to speciate NR-PM_1 components, including organic aerosol (Org), sulfate (SO_4), nitrate (NO_3), ammonium (NH_4), and chloride (Chl). During sampling, ambient air is sampled through an inlet line equipped with a 1 µm cyclone to remove larger particles. The sample air is drawn into the ACSM through a ½-inch stainless steel tube at a flow rate of 3 L/min using an isokinetic sampling line. The particles are then focused by aerodynamic lenses before impacting on the vaporizer heated at ~ 620° C to generate gas phase molecules that are then ionized by the filament. The ionized particles are then detected by the quadrupole mass spectrometer with unit mass resolution.

As described by Ng et al.,(Ng, Herndon, et al. 2011a) aerosol mass concentrations are calculated from the difference between the sample mode and filter mode of the instrument, with each scan comprising 28 filter samples and 28 ambient samples, scanning over 32 seconds each to generate a 30-minute time resolution data points for our analysis.

The instrument's aerodynamic lens was aligned, and the flow calibration was performed before starting the data collection in April 2023. Similarly, the relative ionization efficiency (RIE) calibration(Ng, Herndon, et al. 2011a) was conducted at the beginning of the data collection period, during sampling, and again after 12 months of sampling, which covers the data duration. The RIE values and ammonium nitrate (NH_4NO_3) response factors (RF) were applied to their respective sampling period. During all RIE calibrations, the response factor and RIE for both NO_3 and SO_4 remained stable within a 10% variation across the four calibrations conducted during the campaign.

Ambient black carbon (BC) mass concentration was measured via light absorption at 880 nm with a Magee AE33 aethalometer. The AE33 automatically corrects for filter loading effects using a dual-spot sample collection method; hence, the filter loading effect compensation was not performed during this analysis(Magee scientific 2015). BC source apportionment to distinguish BC from biomass burning and BC from fossil fuel burning was performed using the method described by Sandradewi et al.(Sandradewi

https://doi.org/10.5194/egusphere-2025-1700
Preprint. Discussion started: 9 May 2025

et al. 2008), This approach assumes that the total optical absorption at 950 and 470 nm is the sum of biomass burning and fossil fuel burning fractions.

$PM_{2.5}$ mass concentrations were obtained from a Teledyne T640 $PM_{2.5}$ mass monitor(Teledyne 2016) installed at the U.S. embassy in Kigali. The embassy is located approximately 10 km from the University of Rwanda sampling site. Temperature, relative humidity, wind speed, wind direction, and rainfall data were obtained from a nearby automatic meteorological station owned by Rwanda Meto located at -1.955793 latitude and 30.05641 longitude for the same period of time.

2.3 Data analysis

ACSM data were processed offline using ACSM local v1.6.2.1 in Igor Pro(WaveMetrics 2024). Given that the instrument is equipped with a standard vaporizer, the particle Collection Efficiency (CE) was adjusted to 0.5, as recommended in the literature(Ng, Herndon, et al. 2011b). The CE accounts for particle loss associated with shape-related collection losses at the vaporizer due to the inefficient focusing of non-spherical particles, particle losses resulting from bounce effects of larger particles in the ionization region, and aerodynamic inlet losses as a function of particle diameter(Huffman et al. 2005; Liu et al. 2007; Matthew, Middlebrook, and Onasch 2008; Ng, Herndon, et al. 2011a). The RIE values for NH_4 and SO_4, along with the Response Factor (RF) for NO_3, were automatically loaded into the instrument's data acquisition software and applied to the raw data after each calibration. These factors were also used during post-processing to ensure that the correction factors were consistently applied, ensuring accuracy in the final data analysis.

To ensure the quality of the calibration and instrument performance, the total NR-PM_1 was compared to the $PM_{2.5}$ data obtained from the USA embassy T-640 (see Figure S3 in the supplemental information).

Positive matrix factorization (PMF2.exe) (Paatero and Tapper 1994) and the PMF evaluation tool (PET v.3.06) was used to perform the source apportionment of the organic aerosol for the whole dataset. The PMF-derived source profiles were systematically selected based on the approach explained by Zhang et al.(Zhang et al. 2011)

https://doi.org/10.5194/egusphere-2025-1700
Preprint. Discussion started: 9 May 2025

3. Results and discussion

3.1 NR-PM_1, BC, and $PM_{2.5}$ mass concentration, chemical composition, and seasonal variation.

Figure1 shows the temporal variations in weekly mean concentrations of PM_1 components, including organic aerosols (Org), nitrate (NO_3), sulfate (SO_4), ammonium (NH_4), chloride (Cl), and black carbon (BC). There is a clear seasonal variation in both PM_1 (NR-PM_1 + BC) and $PM_{2.5}$ concentrations, with higher concentrations during the dry seasons (mean PM_1 = 37 µg m^{-3}) than the rainy seasons (mean PM_1 =28 µg m^{-3}). The annual mean concentration in PM_1 was 31 µg m^{-3} whereas $PM_{2.5}$ at the U.S. Embassy in Kigali (denoted as $PM_{2.5}$_UE) was 41 µg m^{-3}. The measured annual mean BC concentration was 4.5 µg/m^3 with a seasonal mean concentration of 5.9 µg/m^3 in the dry seasons and 3.8 µg/m^3 in the rainy seasons.

Concurrent measurements of PM_1 and $PM_{2.5}$ in Kigali showed a strong correlation (R^2 = 0.91) with a slope of 0.65 (See Figure S3 in supporting information). Some of the mass differences between PM_1 and $PM_{2.5}$ can likely be attributed to the impact of dust, which cannot be detected by the ACSM. In addition, site characteristics may play a role, as the US embassy site is classified as an urban near-road site compared to UR/CST site classified as an urban background. The annual mean concentration of $PM_{2.5}$ of 41 µg m^{-3} is comparable with the mean $PM_{2.5}$ concentration of 42.6 µg m^{-3} reported by Gahungu et al. in the same city(Gahungu and Kubwimana 2022b). However, it was higher than the daily mean concentration of $PM_{2.5}$ of 25 µg m^{-3} reported by Kalisa et al. for a 3-month data span in both dry and wet seasons (Kalisa et al. 2018).

Organic aerosols (OA) dominate the PM_1 composition, accounting for 73% of the total mass loading, followed by black carbon (BC) at 16%. Inorganic species collectively contributed 11% of the total PM_1, distributed as follows: NO_3 at 6%, SO_4 at 2%, NH_4 at 2%, and Cl at 1%. The compositions are similar to the findings from a remote area in the same country by Kirago et al.,2022(Kirago et al. 2022) (mean of all seasons): OM at 72%, BC at 4.5%, SO_4 at 12.6%, NO_3 at 4%, and NH_4 at 5.2%. However, SO_4 and NH_4 fractions were 2.6 times lower, and the BC fraction was 4.5 times higher at this urban background site compared to the remote site.

https://doi.org/10.5194/egusphere-2025-1700
Preprint. Discussion started: 9 May 2025

The high contribution of OA to PM_1 mass was also recorded in previous studies in African cities. For example, aircraft measurements in South Africa showed that OA contributed 53% of PM_1 mass, though there was a larger contribution of sulfate (27%) (Brito et al. 2018b). Additionally, filter-based measurements in Dar es Salaam, Tanzania, showed that OA accounted for 68% and inorganic species accounted for 24% of PM_1 mass (Mkoma et al. 2009).

OA dominates the PM_1 composition across both rainy and dry seasons, with a relatively stable fractional contribution: 74% on average during the dry season (mean of JJA and DJF) and 71% during the rainy season (mean of MAM and SON). A similar seasonal composition was also recorded at a remote site in the same country as 72 % and 69% as the mean of the dry and rainy seasons respectively(Kirago et al. 2022)

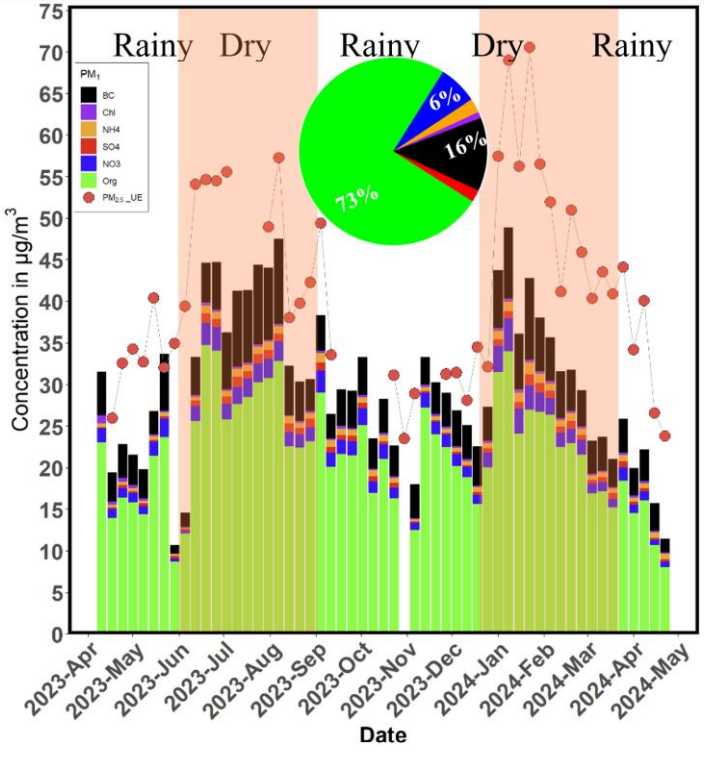

Figure 1: Measured PM_1 and $PM_{2.5}$ in Kigali, Rwanda. Each stacked bar represents the weekly mean concentrations of NR-PM_1 components (SO_4, Org, NO_3, NH4, Chl) and Black Carbon (BC). Red dots indicate $PM_{2.5}$ concentrations measured at the U.S. Embassy, located about 10 km from the ACSM sampling site. The pie chart depicts the overall mean fractional contribution of the total PM1 mass

https://doi.org/10.5194/egusphere-2025-1700
Preprint. Discussion started: 9 May 2025

loading (NR-PM1 + BC). The shaded areas highlight the dry seasons in Rwanda, providing context for seasonal variations in particulate matter.

3.2 Diurnal variations in PM_1 mass and composition

The campaign average diurnal variation in PM_1 components (NR-PM_1 and BC) is presented in Figure 2; seasonal diurnal patterns are shown in Figure S4 in the supporting information. The diurnal patterns show the interplay of emissions and atmospheric processes on pollutant concentrations. These include traffic emissions from busy roads near the sampling site, with 85% of vehicles in Kigali being over 20 years old(Anon 2018; MINEFRA 2018b; Niyibizi et al. 2015; UN Environment 2019). Additionally, emissions from solid fuels contribute significantly, as biomass energy accounts for approximately 85% of the total energy used for cooking in Kigali (MINEFRA 2015; Rwanda Ministry of infrastructure 2018; UN Environment 2019), including emissions from restaurants in the downtown area and densely populated residential areas near the station. Diurnal variability is also influenced by meteorology, including changes in the planetary boundary layer height (PBLH) that is expected to be shallower during night and morning time (6:00 pm to 7:00 am) and expand during the daytime and hence controls the particle mixing volume and concentration.

OA, BC, and NO_3 all exhibit an early morning peak (6:00 am to 9:00 am), a midday decrease, and a second evening peak (6:00 pm to 10:00 pm). The morning peak coincides with increased anthropogenic activities, likely associated with rush hour traffic and cooking activities in the morning. The midday dips in particle concentrations can be attributed to enhanced atmospheric mixing and reduced anthropogenic activities. Daytime increases in the planetary boundary layer height increase the mixing volume and hence reduce the particle concentration during the daytime(Subramanian et al. 2020a). Additionally, higher wind speeds during the daytime contribute to particle dilution (Figure S2 in the Supporting Information). The evening peak is likely due to a combination of decreasing boundary layer height after sunset (typically around 6 pm) and the evening rush hour.

The intra-day variations in concentrations of OA, BC, and NO_3 are large. OA concentrations are ~20 – 25 $\mu g\ m^{-3}$ from midnight to 10 am but fall to ~12 $\mu g\ m^{-3}$ in mid-afternoon. Similarly, BC concentrations change from ~7 $\mu g\ m^{-3}$ to ~2.5 $\mu g\ m^{-3}$ over the same period.

https://doi.org/10.5194/egusphere-2025-1700
Preprint. Discussion started: 9 May 2025

The shape of the diurnal patterns offers insight into potential emissions sources and aerosol processing. The morning peak in BC occurs at 7:00 am. This is one hour earlier than the corresponding morning peak in both OA and NO_3. There are a few possible reasons for the earlier peak in BC. One is that the anthropogenic source mix changes throughout the morning, with the relative impacts of cooking and traffic changing over the period from ~6:00– 10:00 am. A second possibility is that the slight delay in the OA and NO_3 peaks reflects the importance of secondary OA and nitrate formation, and the one-hour delay in their peaks relative to BC is the result of the time needed for chemical conversion from precursor gases to PM components.

OA, BC, and NO_3 all have contributions from local emissions and, therefore, exhibit strong intra-day patterns associated with anthropogenic activities. SO_4, on the other hand, has a much flatter diurnal profile. There is no morning increase in sulfate, though there is a slight midday increase from 10 am to 6 pm. This suggests that SO_4 concentrations in Kigali are regional, reflecting the lack of local SO_4 emissions or SO_2 sources that would contribute to daytime SO_4 formation. For example, there are no coal-fired power plants in Rwanda or nearby areas of neighbouring countries(Global Energy Monitor 2025). Back trajectory analysis (Figure S12) showed that the emissions from the recent activity of the stratovolcano Nyiragongo, which erupted in June 2021 and is located at 1.52°S latitude and 29.25°E longitude in the Democratic Republic of Congo (DRC), did not move toward Kigali(Smithsonia Institute 2025).

https://doi.org/10.5194/egusphere-2025-1700
Preprint. Discussion started: 9 May 2025

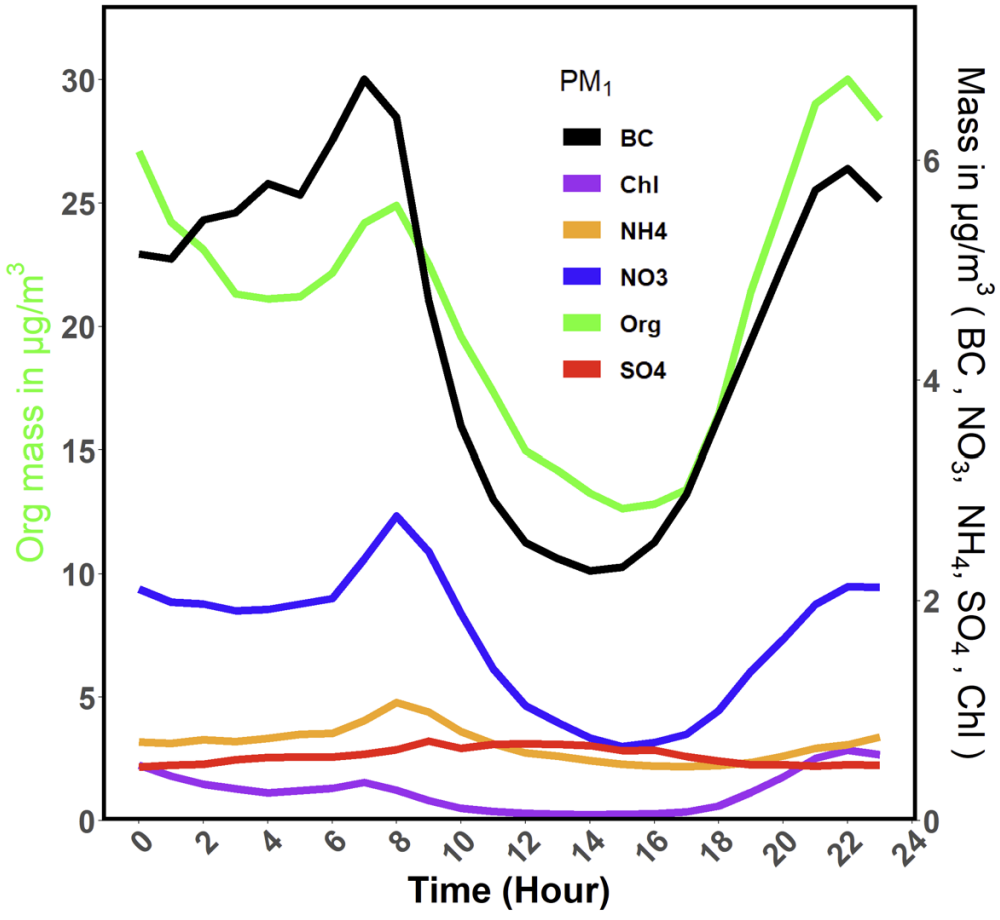

250 Figure 2: Campaign average diurnal profile of NR-PM_1 composition (Chl, NH_4, NO_3, $S0_4$, Org, and BC) with OA plotted on the left y-axis and the other species on the right y-axis.

3.3 Average mass spectrum and contribution of tracer ions

Figure S7 in the Supporting Information shows the campaign-average mass spectrum (MS) measured by the ACSM. The most abundant ions in the mass spectrum are *m/z* 18 (H_20^+) and 44 (CO_2^+). *M/z* 44 is
255 commonly used as a tracer for aged OA(Ng, Canagaratna, et al. 2011a). It accounts for 10.5% of the measured organic aerosol mass whereas *m/z* 18 is for particle water contents.

Other prominent tracer ions in the mass spectrum include *m/z* 43, which has contributions from both $C_3H_7^+$, associated with fresh emissions, and $C_2H_3O^+$, linked to secondary organic aerosol. *M/z* 43 contributed 7% of the OA mass in Kigali. Additional tracer ions such as tracers for urban fresh traffic

https://doi.org/10.5194/egusphere-2025-1700
Preprint. Discussion started: 9 May 2025

emissions (e.g., *m/z* 57 ($C_4H_9^+$)) and fresh biomass burning emissions (*m/z* 60, ($C_2H_4O_2^+$))(Atabakhsh et al. 2023; Christodoulou et al. 2023; Cubison et al. 2011; Werden et al. 2023) together contribute approximately 3.5% of the average PM_1 mass loading.

Inorganic species also contribute significantly to PM_1, with notable nitrate peaks at *m/z* 30 and *m/z* 46, sulfate at *m/z* 48 and *m/z* 64, and ammonium at *m/z* 16 and *m/z* 17. Small peaks at *m/z* 35 and *m/z* 36 indicate chloride makes a minimal contribution (see Figure S7 in the supporting information).

NO_3 accounts for 6% of the total PM_1 mass and consists of both organic and inorganic nitrate species. The ratio of *m/z* 46 to *m/z* 30 is often used to quantify the relative amounts of inorganic and organic nitrate using equation 1(Budisulistiorini et al. 2013; Lanz et al. 2007; Ng, Canagaratna, et al. 2011b).

$$f_{OrgNO_3} = \frac{(R_{ambient} - R_{NH_4NO_3})(1 + R_{OrgNO_3})}{(R_{OrgNO_3} - R_{NH_4NO_3})(1 + R_{ambient})} \quad (1)$$

Here, f_{OrgNO3} is the mass fraction of the total ACSM nitrate that is organic, and R is the ratio of *m/z* 46 to *m/z* 30 for ambient data, NH_4NO_3, and organic nitrates. R_{NH4NO3} can be measured for each instrument during periodic ionization efficiency calibrations. R_{OrgNO3} can be determined from atomizing laboratory standards of organic nitrates, or from literature values. For example, Brito et al.(Brito et al. 2018a) used $R_{OrgNO3} = 0.1$.

An alternative approach, proposed by Day et al(Day et al. 2022), uses a ratio-of-ratios. This method amends equation 1 using R_{NH4NO3}/R_{OrgNO3}. The advantage of this approach is that it accounts for instrument-to-instrument variations in both R_{NH4NO3} and R_{OrgNO3}, instead relying on a constant ratio of ratios for most organic nitrates ($R_{NH4NO3}/R_{OrgNO3} = 2.75$).

The mean $R_{ambient}$ for our data is 0.25 ±0.6, with hourly values ranging from 0.02 to 1.11. Figure S5 in the supporting information shows the results of calculating f_{OrgNO3} both by assuming $R_{OrgNO3} = 0.1$ and using the ratio-of-ratios approach. The former attributes the ambient nitrate as 61% organic, whereas the ratio-of-ratios approach yields f_{OrgNO3} near 100%. Therefore, both approaches indicate that organic nitrates make up a significant fraction of the observed nitrate. The presence of a slight peak in NH_4 during the

https://doi.org/10.5194/egusphere-2025-1700
Preprint. Discussion started: 9 May 2025

morning rush hour (Figure 2) suggests that at least a portion of the nitrate is inorganic, and therefore the f_{OrgNO3} from the ratio-of-ratios approach might be an overestimation.

The diurnal profile of four OA tracer ions (*m/z* 43, 44, 57, and 60) are shown in Figure 3 -. The mass concentrations of all four ions show a similar diurnal pattern as the total OA mass (shown in Figure 2): there is a morning increase in concentration, followed by an afternoon minimum, and concentrations rise again in the evening. While all four of these ions show the same general pattern, the slight differences in their behavior provide insights into PM sources and chemical processing in Kigali.

M/z 60 is a tracer for biomass burning emissions. The morning maximum concentration occurs from 6-7 am and is 1.5 times higher than the minimum concentration observed from 2-4 am. Many people in Kigali (85%) use biomass fuel for cooking(MINEFRA 2015). This morning's increase in *m/z* 60 is likely from cooking activities before the start of the workday.

M/z 57 is commonly used as a tracer for fresh fossil fuel combustion emissions, especially from traffic. The morning peak in *m/z* 57 mass concentration (0.6 µg/m^3) occurs at 7:00 am, with slightly lower concentrations at 8:00 am. This mirrors the diurnal pattern of BC (Fig. 2), which also has a morning maximum at 7 am (6.8 µg/m3). The high concentrations of both BC and *m/z* 57 suggest that the morning rush hour is most intense from 7-8 am. The morning peaks in BC and *m/z* 57 occur slightly after the morning peak in *m/z* 60 (0.3 µg/m^3); this suggests that while both cooking and traffic are important sources in the morning hours, cooking activity starts slightly before traffic volume increases.

M/z 44 is a tracer for oxygenated secondary organic aerosol (SOA). *M/z* 44 also has a morning peak. The morning peak in *m/z* 44 (2.3 µg/m3) occurs at 8:00-9:00 am, after the earlier morning peaks in *m/z* 60 and *m/z* 57. This is suggestive that the morning increase in *m/z* 44 is due to the rapid formation of SOA and that the vehicle and biomass-burning emissions associated with anthropogenic activities are important sources of SOA precursors. Traffic emissions are a well-known source of SOA precursor vapors(Gaita et al. 2014b; Ndamuzi et al. 2024b; Onyango et al. 2024b; REMA 2018b; Subramanian et al. 2020a; UN Environment 2019; West et al. 2020) this is especially true for older vehicles, poorly maintained, or otherwise higher emitting than new vehicles with modern emission control systems(Anon 2018).

M/z 43 is a marker for both primary emissions ($C_3H_7^+$) and SOA ($C_2H_3O^+$). Our quadrupole ACSM has unit mass resolution and, therefore, cannot separate these isobaric ions. The diurnal pattern of *m/z* 43

https://doi.org/10.5194/egusphere-2025-1700
Preprint. Discussion started: 9 May 2025

reflects its dual nature as a marker of primary and secondary OA in Q-ACM. The concentration of *m/z* 43 rises rapidly from 6-7 am, coincident with the morning increase in the concentration of *m/z* 57. This initial increase in *m/z* 43 concentration is likely associated with fresh vehicle emissions. There is a further increase in *m/z* 43 concentration from 8-9 am, coincident with the rapid increase in *m/z* 44 concentration. This further increase in *m/z* 43 is likely due to SOA formation from vehicles and biomass burning emissions.

The temporal patterns of the four marker ions shown in Figure 3 provide insight into sources and atmospheric processes. They all decrease during the afternoon. As with the PM components shown in Figure 2, this decrease is likely due to a combination of changing anthropogenic emissions (e.g., less traffic outside of the morning rush hour), increasing boundary layer height, and faster winds. Concentration rises again in the evening due to a combination of a sinking boundary layer after sunset and evening traffic and cooking activities.

While concentrations of all four tracer ions decrease during the day, the decrease in *m/z* 44 is much smaller than for the other ions. For example, the ratio of the morning peak (7:00 am) to the afternoon trough (2:00 pm) in *m/z* 57 is ~3.3, and the ratio in *m/z* 44 concentration (8:00 am versus 4:00 pm) is ~1.3. This is likely due to the sustained formation of SOA throughout the day. Days in Kigali are consistently sunny (Figure S2 in the Supporting Information), and there is likely a large pool of reactive organic gases available to form SOA. Thus, the impact of boundary-layer driven dilution is larger for ions associated purely with primary emissions (e.g., *m/z* 57) than for ions associated with SOA.

Concentrations of *m/z* 43, 57, and 60 are all higher in the evening hours (~8:00-11:00 pm) than during the morning rush hour. The pattern of traffic and cooking emissions is also reversed in the evening compared to the morning. The late-day increase in the concentrations of *m/z* 57 and 43 precedes the increase in *m/z* 60. This is consistent with expected activity patterns, as people travel home from work before cooking at night.

The mass fractions of each tracer ion, shown in Figure 3b, offer additional insight into the competition between emissions, chemistry, and dilution. The diurnal variation of the mass fraction of *m/z* 57 in OA (f_{57}) is similar to the trend in *m/z* 57 mass. There are morning and evening peaks, with a slightly higher peak in the evening and a midday trough. The ratio of the peaks to the trough is smaller for f_{57} than *m/z*

https://doi.org/10.5194/egusphere-2025-1700
Preprint. Discussion started: 9 May 2025

57 mass (1.5 and 3.3 for f_{57} and *m/z* 57, respectively). This reflects the large role that boundary layer dilution plays on mass concentrations and suggests that traffic activity, and hence emissions, remain high throughout the day.

The diurnal pattern in f_{44} shows a different trend. It rapidly increases after 7 am and peaks at f_{44}= 0.14 at 2:00 pm. The diurnal trend in f_{44} thus indicates that there is rapid formation of SOA, especially in the hours immediately following the high emissions associated with the morning rush hour. After 2 pm, f_{44} gradually decreases as solar intensity diminishes until sunset at 6:00 pm. Taken together, Figs 3a and 3b suggest that there is strong and sustained SOA production throughout the day and that SOA production is fast enough to at least partly counteract the large and rapid boundary layer-driven dilution that occurs during midday.

The diurnal profile of the normalized contribution of *m/z* 43 (f_{43}) remains relatively flat throughout the day. This is a result of the combined role of *m/z* 43 as an indicator for primary and secondary OA. $C_3H_7^+$ is emitted during the morning rush hour and its concentration decreases with the expansion of the boundary layer and oxidation chemistry. $C_2H_3O^+$ increases due to SOA formation through photochemistry. These opposing behaviors result in a relatively constant f_{43} throughout the day.

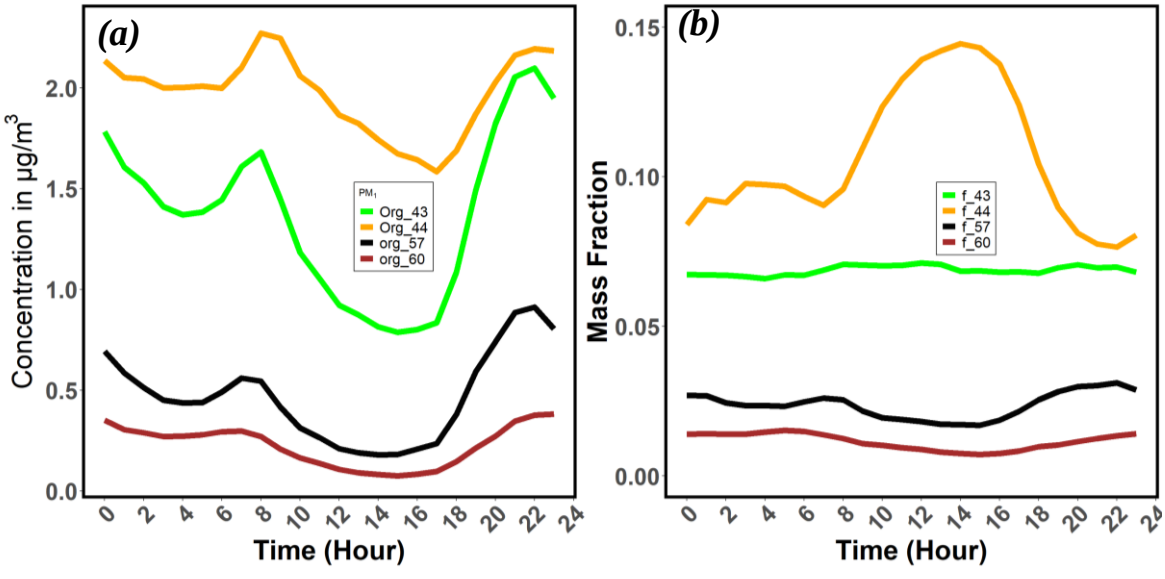

Figure 3: Diurnal variation of individual tracer ions in terms of (a) absolute mass concentrations and (b) mass fraction.

https://doi.org/10.5194/egusphere-2025-1700
Preprint. Discussion started: 9 May 2025

3.4 PM Source apportionment

We performed PMF source apportionment of the OA-only mass spectrum using PMF2.exe and PMF Evaluation Tool version 3.08. The number of factors and source profiles were systematically selected and validated following the recommendations of Ulbrich et al.(Zhang et al. 2011) The most interpretable solutions were chosen based on $Q/Q_{Expected}$ (Q: sum of squared scaled residuals), changes in the total sum of squared scaled residuals with an increasing number of factors, normalized fractional contributions of individual source profiles, and factor spectra comparisons with standard AMS mass spectra(Zhang et al. 2011). Section IV of the Supporting Information shows more details on the PMF analysis, including a comparison of three versus four-factor solutions.

Figure 4(a)shows the mass spectral profiles of deconvolved organic PM_1 source apportionment using PMF. Three factors, Oxygenated Organic Aerosol (OOA), Hydrocarbon-like Organic Aerosol (HOA), and Biomass-Burning Organic Aerosol (BBOA) were identified. The mass spectrum of HOA is characterized by the pronounced hydrocarbon ion series of C_nH_{2n+1} and C_nH_{2n-1}(He et al. 2010). Important peaks in this mass spectrum include *m/z* 41, 43, 55, 57, 69, and 71. In the BBOA mass spectrum, the most prominent peak is at *m/z* 29, with other significant peaks at *m/z* 60, 55, and 43. The OOA mass spectrum is characterized by the large abundance of *m/z* 44.

The HOA, BBOA, and OOA factor profiles show strong similarity to published profiles from ambient deconvolved spectra in other cities, indicating consistency with existing data. When compared to the reference mass spectra, all three factors exhibited strong correlations. The HOA factor had an R^2 value of 0.88 and a slope of 0.85, while the BBOA factor achieved an R^2 of 0.85 and a slope of 0.94. Similarly, the OOA factor profile showed an exceptionally strong correlation with the reference spectra, with an R^2 value of 0.99 (see Figure S10 in the supplementary information document).

PMF results indicate that there are large contributions from both primary and secondary OA. Over the course of the year, the mean contributions of each factor are 45% OOA, 32% HOA, and 23% BBOA. Figure 4b further shows that there is little seasonal variation in source strengths. During the dry season, the mean composition is 47% OOA, 23% BBOA, and 30% HOA, versus 41% OOA, 28% BBOA, and 31% HOA during the wet season. This suggests that the changes in PM_1 mass between the dry and rainy

https://doi.org/10.5194/egusphere-2025-1700
Preprint. Discussion started: 9 May 2025

seasons (Figure 1) are due more to changes in particle loss (e.g., via wet deposition) rather than shifts in emissions, chemical processing, or source strengths.

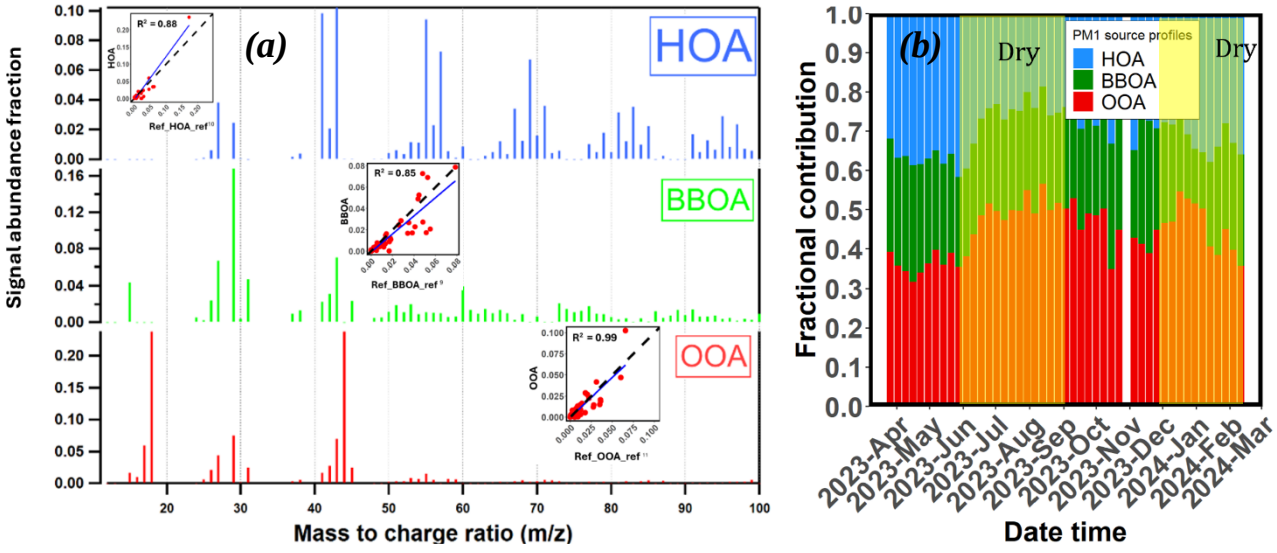

Figure 4: PMF factor profiles (a). The inset scatter plots show the comparison of the source profiles with reference source profiles, and (b) show the seasonal variations in source fractional contributions. In (b), each bar represents the mean relative fractional contribution of the three sources for each week. The yellow shading indicates the two dry seasons.

The diurnal pattern of the source strengths is shown in Figure5. As expected, they mirror the trends in tracer ions shown in Figure3. The OOA factor peaked during the daytime, mirroring f_{44}, underscoring the important role of photochemistry and secondary organic aerosol production at the site. OOA concentrations are less impacted by dilution than HOA and BBOA due to strong daytime SOA production.

https://doi.org/10.5194/egusphere-2025-1700
Preprint. Discussion started: 9 May 2025

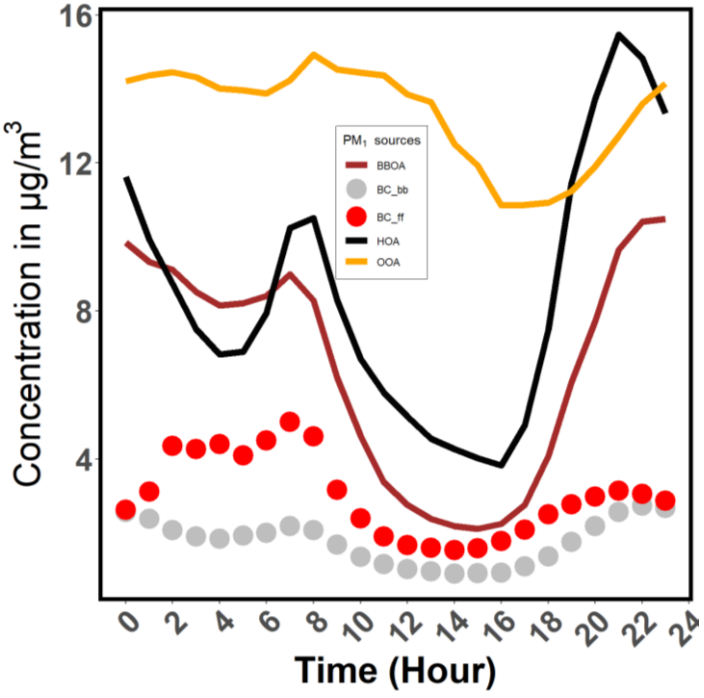

Figure 5: The lines show the diurnal concentrations of OOA, HOA, and BBOA determined from PMF source apportionment of ACSM data. The dots indicate diurnal trends of BC attributable to fossil fuel emissions (red) and biomass burning (grey).

Both BBOA and HOA factors show morning and evening peaks, which mirror anthropogenic activities. The morning peak in BBOA occurs before the morning peak in HOA associated with rush hour traffic. In the afternoon, the trend is reversed, with HOA concentrations increasing and reaching an evening peak before BBOA. For both BBOA and HOA, the evening peak in concentrations is larger than the morning peak. Throughout most of the day, concentrations of HOA are smaller than concentrations of OOA. However, during the evening peak from ~6:00-10:00 pm, HOA concentrations are larger than OOA concentrations.

BC contributes ~16% of the PM_1 mass. Using the algorithm developed by Sandradewi et al.(Sandradewi et al. 2008), BC was decomposed into BC from fossil fuel combustion (BC_ff) and BC from biomass burning (BC_bb) fractions. The annual mean BC measured in Kigali consists of 59% BC_ff and 41% BC_bb. Figure S6 in the supporting information shows that there is minimal seasonal variation in BC source apportionment. Across all seasons, BC_ff contributed 55–63% of the total BC mass loading, with BC_bb contributing 37-45% of observed BC mass. These results are contrary to the BC composition

https://doi.org/10.5194/egusphere-2025-1700
Preprint. Discussion started: 9 May 2025

recorded at the Rwanda Climate Observatory (RCO), which is located in a remote area. There, BC was 8-13% BC_ff and 87-92% BC_bb(Andersson et al. 2020a; Kirago et al. 2022), this difference may be attributed to the site characteristics where RCO is a remote site compared to the measurement at this urban site that is likely to be influenced by the anthropogenic emissions from cooking and traffic.

The diurnal patterns of both BC_ff and BC_bb are shown alongside the PMF analysis in Figure 5. Overall, the diurnal patterns of BC_ff and BC_bb are similar to the diurnal patterns in HOA and BBOA, respectively. The BC_ff component, represented by the red markers, exhibits pronounced peaks during the morning (6:00–9:00 am) and evening (5:00–9:00 pm) hours, corresponding to increased vehicular emissions during rush hours under the influence of a shallower planetary boundary layer. In contrast, the BC_bb component, depicted by the grey markers, shows relatively consistent levels throughout the day, with slight increases observed during the late evening (8:00–10:00 PM) and early morning (6:00–10:00 AM) hours.

There was a positive correlation between hourly BC and BBOA (R^2 = 0.86), BC_bb and BBOA (R^2 = 0.86), and BC and *m/z* 60 (R^2 = 0.94). Similarly, the HOA factor showed a linear relationship with BC (R^2 = 0.73), BC_ff (R^2 = 0.61), and *m/z* 57 (R^2 = 0.95), (see S10 and S11 in the supplement information) indicating significant contributions from fossil fuel combustion and biomass burning to the total PM mass at the site.

While there is limited data on air pollution sources in other East African countries, our results are consistent with the past literature. In Mbarara, Uganda, a neighboring country of Rwanda, elemental $PM_{2.5}$ composition analysis and PMF revealed large contributions of traffic emissions and biomass burning, contributing 36% and 28% of the total $PM_{2.5}$ mass, respectively (Onyango et al. 2024b). In Nairobi, Kenya, Gauta et al. (Gaita et al. 2014b) reported that traffic-related emissions accounted for 39% of the total $PM_{2.5}$ mass.

In Western African countries, primary organic aerosols (POA) are also major contributors to $PM_{2.5}$ mass. For instance, in Bamako, Mali, POA contributes 60–65% of the total $PM_{2.5}$ mass. Similarly, in Dakar, Senegal, traffic emissions (including motor vehicle tailpipe emissions and resuspended road dust) account for 45–49% of the total $PM_{2.5}$ mass loading (Doumbia et al. 2023; UN Environment 2018, 2019).

https://doi.org/10.5194/egusphere-2025-1700
Preprint. Discussion started: 9 May 2025

Different countries in Eastern Africa are implementing various measures to reduce PM emissions. For example, in the transportation sector, Rwanda has adopted electric mobility policies to reduce traffic-related PM emissions(Republic of Rwanda 2021). A 2021 strategic paper on electric mobility adaptation by the Ministry of Infrastructure(Republic of Rwanda 2021) outlines import and excise duty exemptions on electric vehicles (EVs), spare parts, investments in charging infrastructure, and access to high-occupancy vehicle lanes for EVs. Additionally, this strategy applies to a carbon tax on high-emission vehicles (old petrol-powered vehicles) to discourage the use and importation of older and polluting vehicles. This strategy introduced tax exemptions on LPG to improve the affordability and adoption of EVs(Republic of Rwanda 2021). To enhance compliance, the government of Rwanda has established motor vehicle inspection centers, requiring commercial vehicles to undergo biannual inspections and personal vehicles to be inspected annually. This initiative ensures that older, high-PM-emitting vehicles are monitored and regulated. Research by Subramanian et al.(Subramanian et al. 2020b) shows that Rwanda's car-free initiatives, such as car-free zones and car-free days, can successfully reduce $PM_{2.5}$ concentrations by 10-12 µg/m³ and black carbon (BC) by 1 µg/m³, demonstrating the effectiveness of vehicle emissions reductions in PM concentrations.

In the household energy sector, Rwanda is actively working to reduce PM emissions from biomass cooking by lowering biomass energy use from 85% to 44%(Republic of Rwanda 2022). The 2022 ministerial guidelines on clean cooking technologies promote the adoption of LPG, biogas, liquid fuels, and improved clean-burning cookstoves to reduce indoor and outdoor PM emissions from biomass combustion hence the large-scale distribution of low-emission cookstoves to rural communities further supports this transition(Republic of Rwanda 2022).

For industrial PM emissions, the eastern African community developed different air emission Standards for instance EAS 750:2010, EAC 751:2010, and EAC 1047:2022, which regulate air ambient, cement factory, and tailpipe emissions respectively (Rwanda Standard Board 2010). This effort is expected to improve air quality and reduce the impact of air pollution on public health, the environment, and climate change.

https://doi.org/10.5194/egusphere-2025-1700
Preprint. Discussion started: 9 May 2025

4. Conclusion

The measurements presented here show that PM_1 in Kigali is impacted by high primary emissions of BC and OA, along with strong secondary production of OA and nitrate. This is consistent with Rwanda being a nation with a relatively old and higher-emitting vehicle fleet, high usage of solid biomass fuels for cooking, and high solar insolation.

The transport sector in Rwanda is dominated by old vehicles imported from other countries. Rwanda's registered motor vehicles, including two-wheeled taxis ("motos") but excluding security organs and government vehicles, totaled 191,015 in 2017 and 264,524 in 2020. Of these, only 15% were new vehicles, while the remaining 85% were imported used vehicles, 95% of which were manufactured before 2005(Niyibizi et al. 2015; REMA 2018b; Republic of Rwanda 2021; UN Environment 2018, 2019). While we do not have specific emissions measurements for the vehicle fleet, the ambient data presented here suggest that vehicles in Rwanda are high emitters of both BC and OA. Additionally, these vehicle emissions contribute precursor vapors for SOA production.

In Rwanda, as in most Eastern African countries, biomass (e.g., charcoal, wood, and biogas derived from waste materials) accounts for more than 80% of total energy consumption (MINEFRA 2018b). Our analyses show that biomass burning, even in urban Kigali, contributes 23% of OA and 41% of BC. Some of the OA and BC attributable to biomass burning are emitted locally, as evidenced by the morning and evening peaks in BBOA and BC_bb. However, the morning and evening enhancements in BBOA and BC_bb are relatively small, and there are also high concentrations of BBOA and BC_bb overnight (e.g., from 12:00 am to 4:00 am). Anderson et al. (2020) and Kirago et al.(2022) measured a mean concentration of ~0.5 μg m^{-3} at the remote Rwanda Climate Observatory; this BC was 91% attributed to biomass burning. If we assume that the Rwanda Climate Observatory measurements represent a regional concentration of biomass-related BC, then about one-third of the biomass-burning BC in Kigali is from regional sources.

There are modest seasonal variations in PM_1 mass concentrations, with about 10% higher concentrations of both PM_1 and $PM_{2.5}$ during the dry season. Source apportionment analysis of both OA and BC shows

https://doi.org/10.5194/egusphere-2025-1700
Preprint. Discussion started: 9 May 2025

smaller variations in source strengths across seasons. This suggests that the main reason for higher PM concentrations in the dry seasons is a reduction in wet deposition, rather than increased source strengths. However, there remains the possibility that there exist season-dependent shifts in emissions sources. For example, the rainy seasons have a higher fraction of BC from biomass-burning sources than the dry seasons. This may be due to biomass burning for agricultural residue disposal or because of transported emissions from open burning in the northern and southern regions of Rwanda(Andersson et al. 2020b).

While regional cooperation frameworks exist, weak enforcement remains a major challenge in addressing transboundary PM pollution. Strengthening compliance requires the establishment of a legally binding regional agreement with clear PM reduction targets and penalties for non-compliance. Prioritizing a joint regional PM monitoring network would enable real-time tracking of PM sources, supporting evidence-based enforcement. Additionally, empowering cross-border regulatory bodies to conduct independent audits, inspections, and enforcement actions is essential to ensure compliance with PM standards. Strengthening regional funding mechanisms for clean energy transitions and emission reduction projects targeting PM sources, such as biomass burning, industrial activities, and vehicle emissions, would provide critical financial support while fostering collaboration among governments, industries, and environmental agencies across the region.

5. Data availability.

All data presented in this work can be obtained by directly contacting the corresponding author at apresto@andrew.cmu.edu upon request. Data will also be posted to a publicly available server (https://kilthub.cmu.edu/) upon final acceptance.

6. Competing interests.

The authors declare that they have no conflict of interest.

https://doi.org/10.5194/egusphere-2025-1700
Preprint. Discussion started: 9 May 2025

7. Author contribution

The experimental design was done by AAP, ALR, and TH. Data collection was carried out by AAP and TH. TH performed the data analysis and compiled the instrumental data. TH, AAP, and ALR wrote the paper, with all authors contributing significantly to the interpretation of the results, discussions, and finalization of the paper.

8. Acknowledgments

This work was funded by National Science Foundation Grants 2420751 and 2020666 and the Steinbrenner Institute for Environmental Education and Research at Carnegie Mellon University. We thank the Rwanda Space Agency, and Earth and Space Science Division, for providing the Q-ACSM and AE33 instrument data used in this study. We also extend our gratitude to the Rwanda Space Agency technical team (Dr. Ntwali Didier, Mr. Olivier Shyaka, Mr. Gaston Munyampundu, Mr. Jacques Nshuti, Mr. Eric Byiringiro, and Mr. Emmanuel Iradukunda) from the Rwanda Climate Observatory Project for their technical support and assistance with instrument operation.

9. References

: Health Effects Institute. 2022. 'The State of Air Quality and Health Impact in Africa'.

Abera, Asmamaw, Johan Friberg, Christina Isaxon, Michael Jerrett, Ebba Malmqvist, Cheryl Sjöström, Tahir Taj, and Ana Maria Vargas. 2021. 'Air Quality in Africa: Public Health Implications'. *Annual Review of Public Health Annu. Rev. Public Health* 42:193–210. doi: 10.1146/annurev-publhealth.

AirNow. 2025. 'Air Pollution Measurement'. *Https://Gispub.Epa.Gov/Airnow/?Xmin=-45840156.57887686&xmax=21786434.0780193&ymin=-13098308.031629872&ymax=18640792.097272202&contours=none&monitors=pm25*.

Andersson, August, Elena N. Kirillova, Stefano Decesari, Langley Dewitt, Jimmy Gasore, Katherine E. Potter, Ronald G. Prinn, Maheswar Rupakheti, Jean De Dieu Ndikubwimana, Julius Nkusi, and Bonfils Safari. 2020a. 'Seasonal Source Variability of Carbonaceous Aerosols at the Rwanda Climate Observatory'. *Atmospheric Chemistry and Physics* 20(8):4561–73. doi: 10.5194/acp-20-4561-2020.

https://doi.org/10.5194/egusphere-2025-1700
Preprint. Discussion started: 9 May 2025

Andersson, August, Elena N. Kirillova, Stefano Decesari, Langley Dewitt, Jimmy Gasore, Katherine E. Potter, Ronald G. Prinn, Maheswar Rupakheti, Jean De Dieu Ndikubwimana, Julius Nkusi, and Bonfils Safari. 2020b. 'Seasonal Source Variability of Carbonaceous Aerosols at the Rwanda Climate Observatory'. *Atmospheric Chemistry and Physics* 20(8):4561–73. doi: 10.5194/acp-20-4561-2020.

Anon. 2018. *Republic Of Rwanda Ministry Of Infrastructure*.

Atabakhsh, Samira, Laurent Poulain, Gang Chen, Francesco Canonaco, André S. H. Prévôt, Mira Pöhlker, Alfred Wiedensohler, and Hartmut Herrmann. 2023. 'A 1-Year Aerosol Chemical Speciation Monitor (ACSM) Source Analysis of Organic Aerosol Particle Contributions from Anthropogenic Sources after Long-Range Transport at the TROPOS Research Station Melpitz'. *Atmospheric Chemistry and Physics* 23(12):6963–88. doi: 10.5194/acp-23-6963-2023.

Brito, Joel, Evelyn Freney, Pamela Dominutti, Agnes Borbon, Sophie L. Haslett, Anneke M. Batenburg, Aurelie Colomb, Regis Dupuy, Cyrielle Denjean, Frederic Burnet, Thierry Bourriane, Adrien Deroubaix, Karine Sellegri, Stephan Borrmann, Hugh Coe, Cyrille Flamant, Peter Knippertz, and Alfons Schwarzenboeck. 2018a. 'Assessing the Role of Anthropogenic and Biogenic Sources on PM1 over Southern West Africa Using Aircraft Measurements'. *Atmospheric Chemistry and Physics* 18(2):757–72. doi: 10.5194/acp-18-757-2018.

Brito, Joel, Evelyn Freney, Pamela Dominutti, Agnes Borbon, Sophie L. Haslett, Anneke M. Batenburg, Aurelie Colomb, Regis Dupuy, Cyrielle Denjean, Frederic Burnet, Thierry Bourriane, Adrien Deroubaix, Karine Sellegri, Stephan Borrmann, Hugh Coe, Cyrille Flamant, Peter Knippertz, and Alfons Schwarzenboeck. 2018b. 'Assessing the Role of Anthropogenic and Biogenic Sources on PM1 over Southern West Africa Using Aircraft Measurements'. *Atmospheric Chemistry and Physics* 18(2):757–72. doi: 10.5194/acp-18-757-2018.

Budisulistiorini, Sri Hapsari, Manjula R. Canagaratna, Philip L. Croteau, Wendy J. Marth, Karsten Baumann, Eric S. Edgerton, Stephanie L. Shaw, Eladio M. Knipping, Douglas R. Worsnop, John T. Jayne, Avram Gold, and Jason D. Surratt. 2013. 'Real-Time Continuous Characterization of Secondary Organic Aerosol Derived from Isoprene Epoxydiols in Downtown Atlanta, Georgia, Using the Aerodyne Aerosol Chemical Speciation Monitor'. *Environmental Science and Technology* 47(11):5686–94. doi: 10.1021/es400023n.

Christodoulou, Aliki, Iasonas Stavroulas, Mihalis Vrekoussis, Maximillien Desservettaz, Michael Pikridas, Elie Bimenyimana, Jonilda Kushta, Matic Ivančič, Martin Rigler, Philippe Goloub, Konstantina Oikonomou, Roland Sarda-Estève, Chrysanthos Savvides, Charbel Afif, Nikos Mihalopoulos, Stéphane Sauvage, and Jean Sciare. 2023. 'Ambient Carbonaceous Aerosol Levels in Cyprus and the Role of Pollution Transport from the Middle East'. *Atmospheric Chemistry and Physics* 23(11):6431–56. doi: 10.5194/acp-23-6431-2023.

Cubison, M. J., A. M. Ortega, P. L. Hayes, D. K. Farmer, D. Day, M. J. Lechner, W. H. Brune, E. Apel, G. S. Diskin, J. A. Fisher, H. E. Fuelberg, A. Hecobian, D. J. Knapp, T. Mikoviny, D. Riemer, G. W. Sachse, W. Sessions, R. J. Weber, A. J. Weinheimer, A. Wisthaler, and J. L. Jimenez. 2011. 'Effects of Aging on Organic Aerosol from Open Biomass Burning Smoke in Aircraft and Laboratory Studies'. *Atmospheric Chemistry and Physics* 11(23):12049–64. doi: 10.5194/acp-11-12049-2011.

https://doi.org/10.5194/egusphere-2025-1700
Preprint. Discussion started: 9 May 2025

Day, Douglas A., Pedro Campuzano-Jost, Benjamin A. Nault, Brett B. Palm, Weiwei Hu, Hongyu Guo, Paul J. Wooldridge, Ronald C. Cohen, Kenneth S. Docherty, J. Alex Huffman, Suzane S. De Sá, Scot T. Martin, and Jose L. Jimenez. 2022. 'A Systematic Re-Evaluation of Methods for Quantification of Bulk Particle-Phase Organic Nitrates Using Real-Time Aerosol Mass Spectrometry'. *Atmospheric Measurement Techniques* 15(2):459–83. doi: 10.5194/amt-15-459-2022.

Dhammapala, Ranil. 2019. 'Analysis of Fine Particle Pollution Data Measured at 29 US Diplomatic Posts Worldwide'. *Atmospheric Environment* 213:367–76. doi: 10.1016/j.atmosenv.2019.05.070.

Doumbia, Thierno, Catherine Liousse, Marie Roumy Ouafo-Leumbe, Seydi Ababacar Ndiaye, Eric Gardrat, Corinne Galy-Lacaux, Cyril Zouiten, Véronique Yoboué, and Claire Granier. 2023. 'Source Apportionment of Ambient Particulate Matter (PM) in Two Western African Urban Sites (Dakar in Senegal and Bamako in Mali)'. *Atmosphere* 14(4). doi: 10.3390/atmos14040684.

Environmental Compliance institute. 2018. *Kigali City Air Quality Policy and Regulatory Situational Analysis A Report Published by UN Environment in Collaboration with Environmental Compliance Institute*.

Fisher, Samantha, David C. Bellinger, Maureen L. Cropper, Pushpam Kumar, Agnes Binagwaho, Juliette Biao Koudenoukpo, Yongjoon Park, Gabriella Taghian, and Philip J. Landrigan. 2021. 'Air Pollution and Development in Africa: Impacts on Health, the Economy, and Human Capital'. *The Lancet Planetary Health* 5(10):e681–88. doi: 10.1016/S2542-5196(21)00201-1.

Gahungu, Paterne, and Jean Remy Kubwimana. 2022a. 'Trend Analysis and Forecasting Air Pollution in Rwanda'.

Gahungu, Paterne, and Jean Remy Kubwimana. 2022b. 'Trend Analysis and Forecasting Air Pollution in Rwanda'.

Gaita, S. M., J. Boman, M. J. Gatari, J. B. C. Pettersson, and S. Janhäll. 2014a. 'Source Apportionment and Seasonal Variation of PM2.5 in a Sub-Saharan African City: Nairobi, Kenya'. *Atmospheric Chemistry and Physics* 14(18):9977–91. doi: 10.5194/acp-14-9977-2014.

Gaita, S. M., J. Boman, M. J. Gatari, J. B. C. Pettersson, and S. Janhäll. 2014b. 'Source Apportionment and Seasonal Variation of PM2.5 in a Sub-Saharan African City: Nairobi, Kenya'. *Atmospheric Chemistry and Physics* 14(18):9977–91. doi: 10.5194/acp-14-9977-2014.

GBD. 2024. 'Global Burden Deseases'. *Https://Vizhub.Healthdata.Org/Gbd-Compare/#*.

Global Energy Monitor. 2025. 'Worldwide Coal Plants '. *Https://Globalenergymonitor.Org/Projects/Global-Coal-Plant-Tracker/Tracker/*.

He, L. Y., Y. Lin, X. F. Huang, S. Guo, L. Xue, Q. Su, M. Hu, S. J. Luan, and Y. H. Zhang. 2010. 'Characterization of High-Resolution Aerosol Mass Spectra of Primary Organic Aerosol Emissions from Chinese Cooking and Biomass Burning'. *Atmospheric Chemistry and Physics* 10(23):11535–43. doi: 10.5194/acp-10-11535-2010.

Health Effects Institute. 2022. 'The State of Air Quality and Health Impacts in Africa.'

Huffman, J. Alex, John T. Jayne, Frank Drewnick, Allison C. Aiken, Timothy Onasch, Douglas R. Worsnop, and Jose L. Jimenez. 2005. 'Design, Modeling, Optimization, and Experimental Tests of a Particle Beam Width Probe for the

https://doi.org/10.5194/egusphere-2025-1700
Preprint. Discussion started: 9 May 2025

Aerodyne Aerosol Mass Spectrometer'. *Aerosol Science and Technology* 39(12):1143–63. doi: 10.1080/02786820500423782.

Kalisa, Egide, Vincent Kuuire, and Matthew Adams. 2023. 'Children's Exposure to Indoor and Outdoor Black Carbon and Particulate Matter Air Pollution at School in Rwanda, Central-East Africa'. *Environmental Advances* 11. doi: 10.1016/j.envadv.2022.100334.

Kalisa, Egide, Edward G. Nagato, Elias Bizuru, Kevin C. Lee, Ning Tang, Stephen B. Pointing, Kazuichi Hayakawa, Stephen D. J. Archer, and Donnabella C. Lacap-Bugler. 2018. 'Characterization and Risk Assessment of Atmospheric PM 2.5 and PM 10 Particulate-Bound PAHs and NPAHs in Rwanda, Central-East Africa'. *Environmental Science and Technology* 52(21):12179–87. doi: 10.1021/acs.est.8b03219.

Kigali city. 2024a. 'Kigali City Population'. *Https://Www.Kigalicity.Gov.Rw/about/Overview*.

Kigali city. 2024b. 'Kigali City Population(Last Accessed: Nov 2024).' *Https://Www.Kigalicity.Gov.Rw/about/Overview*.

Kirago, Leonard, Örjan Gustafsson, Samuel M. Gaita, Sophie L. Haslett, H. Langley Dewitt, Jimmy Gasore, Katherine E. Potter, Ronald G. Prinn, Maheswar Rupakheti, Jean De Dieu Ndikubwimana, Bonfils Safari, and August Andersson. 2022. 'Atmospheric Black Carbon Loadings and Sources over Eastern Sub-Saharan Africa Are Governed by the Regional Savanna Fires'. *Environmental Science and Technology* 56(22):15460–69. doi: 10.1021/acs.est.2c05837.

Langley Dewitt, H., Jimmy Gasore, Maheswar Rupakheti, Katherine E. Potter, Ronald G. Prinn, Jean De Dieu Ndikubwimana, Julius Nkusi, and Bonfils Safari. 2019. 'Seasonal and Diurnal Variability in O3, Black Carbon, and CO Measured at the Rwanda Climate Observatory'. *Atmospheric Chemistry and Physics* 19(3):2063–78. doi: 10.5194/acp-19-2063-2019.

Lanz, V. A., M. R. Alfarra, U. Baltensperger, B. Buchmann, C. Hueglin, and A. S. H. Prévôt. 2007. *Source Apportionment of Submicron Organic Aerosols at an Urban Site by Factor Analytical Modelling of Aerosol Mass Spectra*. Vol. 7.

Liu, Peter S. K., Rensheng Deng, Kenneth A. Smith, Leah R. Williams, John T. Jayne, Manjula R. Canagaratna, Kori Moore, Timothy B. Onasch, Douglas R. Worsnop, and Terry Deshler. 2007. 'Transmission Efficiency of an Aerodynamic Focusing Lens System: Comparison of Model Calculations and Laboratory Measurements for the Aerodyne Aerosol Mass Spectrometer'. *Aerosol Science and Technology* 41(8):721–33. doi: 10.1080/02786820701422278.

Magee scientific. 2015. *Aethalometer ® Model AE33 User Manual*.

Matthew, Brendan M., Ann M. Middlebrook, and Timothy B. Onasch. 2008. 'Collection Efficiencies in an Aerodyne Aerosol Mass Spectrometer as a Function of Particle Phase for Laboratory Generated Aerosols'. *Aerosol Science and Technology* 42(11):884–98. doi: 10.1080/02786820802356797.

McFarlane, Celeste, Paulson Kasereka Isevulambire, Raymond Sinsi Lumbuenamo, Arnold Murphy Elouma Ndinga, Ranil Dhammapala, Xiaomeng Jin, V. Faye McNeill, Carl Malings, R. Subramanian, and Daniel M. Westervelt. 2021. 'First Measurements of Ambient Pm2.5 in Kinshasa, Democratic Republic of Congo and Brazzaville, Republic of Congo Using Field-Calibrated Low-Cost Sensors'. *Aerosol and Air Quality Research* 21(7). doi: 10.4209/aaqr.200619.

Miller, Joshua, and Lingzhi Jin. 2018. *Global Progress toward Soot-Free Diesel Vehicles in 2018*.

MINEFRA. 2015. *Republic Of Rwanda Ministry Of Infrastructure Rwanda Energy Policy*.

https://doi.org/10.5194/egusphere-2025-1700
Preprint. Discussion started: 9 May 2025

MINEFRA. 2018a. *ENERGY SECTOR STRATEGIC PLAN*.

MINEFRA. 2018b. *Republic Of Rwanda Ministry Of Infrastructure Energy Sector Strategic Plan*.

Mkoma, Stelyus L., Willy Maenhaut, Xuguang Chi, Wan Wang, and Nico Raes. 2009. 'Characterisation of PM10 Atmospheric Aerosols for the Wet Season 2005 at Two Sites in East Africa'. *Atmospheric Environment* 43(3):631–39. doi: 10.1016/j.atmosenv.2008.10.008.

Ndamuzi, Egide, Rachel Akimana, Paterne Gahungu, and Elie Bimenyimana. 2024a. 'Modeling and Characterization of Fine Particulate Matter Dynamics in Bujumbura Using Low-Cost Sensors'. *Journal of Applied Mathematics and Physics* 12(01):256–67. doi: 10.4236/jamp.2024.121020.

Ndamuzi, Egide, Rachel Akimana, Paterne Gahungu, and Elie Bimenyimana. 2024b. 'Modeling and Characterization of Fine Particulate Matter Dynamics in Bujumbura Using Low-Cost Sensors'. *Journal of Applied Mathematics and Physics* 12(01):256–67. doi: 10.4236/jamp.2024.121020.

Ng, N. L., M. R. Canagaratna, J. L. Jimenez, Q. Zhang, I. M. Ulbrich, and D. R. Worsnop. 2011a. 'Real-Time Methods for Estimating Organic Component Mass Concentrations from Aerosol Mass Spectrometer Data'. *Environmental Science and Technology* 45(3):910–16. doi: 10.1021/es102951k.

Ng, N. L., M. R. Canagaratna, J. L. Jimenez, Q. Zhang, I. M. Ulbrich, and D. R. Worsnop. 2011b. 'Real-Time Methods for Estimating Organic Component Mass Concentrations from Aerosol Mass Spectrometer Data'. *Environmental Science and Technology* 45(3):910–16. doi: 10.1021/es102951k.

Ng, N. L., S. C. Herndon, A. Trimborn, M. R. Canagaratna, P. L. Croteau, T. B. Onasch, D. Sueper, D. R. Worsnop, Q. Zhang, Y. L. Sun, and J. T. Jayne. 2011a. 'An Aerosol Chemical Speciation Monitor (ACSM) for Routine Monitoring of the Composition and Mass Concentrations of Ambient Aerosol'. *Aerosol Science and Technology* 45(7):780–94. doi: 10.1080/02786826.2011.560211.

Ng, N. L., S. C. Herndon, A. Trimborn, M. R. Canagaratna, P. L. Croteau, T. B. Onasch, D. Sueper, D. R. Worsnop, Q. Zhang, Y. L. Sun, and J. T. Jayne. 2011b. 'An Aerosol Chemical Speciation Monitor (ACSM) for Routine Monitoring of the Composition and Mass Concentrations of Ambient Aerosol'. *Aerosol Science and Technology* 45(7):780–94. doi: 10.1080/02786826.2011.560211.

Niyibizi, Ananie, Jean Baptiste Nduwayezu, Theoneste Ishimwe, and Benjamin Ngirabakunzi. 2015. 'Quantification of Air Pollution in Kigali City and Its Environmental and Socio-Economic Impact in Rwanda'. *American Journal of Environmental Engineering* 5:106–19. doi: 10.5923/j.ajee.20150504.03.

Onyango, Silver, Crystal M. North, Hatem A. Ellaithy, Paul Tumwesigye, Choong Min Kang, Vasileios Matthaios, Martin Mukama, Nuriat Nambogo, J. Mikhail Wolfson, Stephen Ferguson, Stephen Asiimwe, Lynn Atuyambe, Data Santorino, David C. Christiani, and Petros Koutrakis. 2024a. 'Ambient PM2.5 Temporal Variation and Source Apportionment in Mbarara, Uganda'. *Aerosol and Air Quality Research* 24(4). doi: 10.4209/aaqr.230203.

Onyango, Silver, Crystal M. North, Hatem A. Ellaithy, Paul Tumwesigye, Choong Min Kang, Vasileios Matthaios, Martin Mukama, Nuriat Nambogo, J. Mikhail Wolfson, Stephen Ferguson, Stephen Asiimwe, Lynn Atuyambe, Data Santorino,

https://doi.org/10.5194/egusphere-2025-1700
Preprint. Discussion started: 9 May 2025

David C. Christiani, and Petros Koutrakis. 2024b. 'Ambient PM2.5 Temporal Variation and Source Apportionment in Mbarara, Uganda'. *Aerosol and Air Quality Research* 24(4). doi: 10.4209/aaqr.230203.

openaq. 2025. 'Air Pollution Monitoring Map'. *Https://Explore.Openaq.Org/?Parameter=pm25#1/24.6/55.8*.

Paatero, Pentti, and Unto Tapper. 1994. 'Positive Matrix Factorization: A Non-negative Factor Model with Optimal Utilization of Error Estimates of Data Values'. *Environmetrics* 5(2):111–26. doi: 10.1002/env.3170050203.

REMA. 2018a. *Inventory of Sources of Air Pollution in Rwanda Determination of Future Trends and Development of a National Air Quality Control Strategy*.

REMA. 2018b. *Rwanda Environment Management Authority Inventory of Sources of Air Pollution in Rwanda Determination of Future Trends and Development of a National Air Quality Control Strategy Rwanda Environment Management Authority*.

Republic of Rwanda. 2021. *Electric Mobility Adaptation in Rwanda*.

Republic of Rwanda. 2022. 'Ministerial_Guidelines_for_Clean_Cooking_Technologies'.

Rwanda Meteo. 2025. 'Rwanda Climatology Last Accessed: Nov 2024)'. *Https://Www.Meteorwanda.Gov.Rw/Index.Php?Id=2*.

Rwanda Ministry of infrastructure. 2018. *ENERGY SECTOR STRATEGIC PLAN*.

Rwanda Standard Board. 2010. 'Emission to the Air by Cement Factories, RS EAC 750:2010 (Last Accessed: April 2024), 2010.' Retrieved 22 April 2025 (https://portal.rsb.gov.rw/webstore_preview.php?id=ODY3RkJrTndaM0EzcA).

Sandradewi, Jisca, Andre S. H. Prévôt, Sönke Szidat, Nolwenn Perron, M. Rami Alfarra, Valentin A. Lanz, Ernest Weingartner, and U. R. S. Baltensperger. 2008. 'Using Aerosol Light Abosrption Measurements for the Quantitative Determination of Wood Burning and Traffic Emission Contribution to Particulate Matter'. *Environmental Science and Technology* 42(9):3316–23. doi: 10.1021/es702253m.

Singh, Ajit, David Ng'ang'a, Michael J. Gatari, Abel W. Kidane, Zinabu A. Alemu, Ndawula Derrick, Mbujje J. Webster, Suzanne E. Bartington, G. Neil Thomas, William Avis, and Francis D. Pope. 2021a. 'Air Quality Assessment in Three East African Cities Using Calibrated Low-Cost Sensors with a Focus on Road-Based Hotspots'. *Environmental Research Communications* 3(7). doi: 10.1088/2515-7620/ac0e0a.

Singh, Ajit, David Ng'ang'a, Michael J. Gatari, Abel W. Kidane, Zinabu A. Alemu, Ndawula Derrick, Mbujje J. Webster, Suzanne E. Bartington, G. Neil Thomas, William Avis, and Francis D. Pope. 2021b. 'Air Quality Assessment in Three East African Cities Using Calibrated Low-Cost Sensors with a Focus on Road-Based Hotspots'. *Environmental Research Communications* 3(7). doi: 10.1088/2515-7620/ac0e0a.

Smithsonia Institute. 2025. 'Volcanic Activity in Africa(Last Access: Feb 2025)'. *Https://Volcano.Si.Edu/Volcano.Cfm?Vn=223030*.

Subramanian, R., Abdou Safari Kagabo, Valerien Baharane, Sandrine Guhirwa, Claver Sindayigaya, Carl Malings, Nathan J. Williams, Egide Kalisa, Haofan Li, Peter Adams, Allen L. Robinson, H. Langley DeWitt, Jimmy Gasore, and Paulina

https://doi.org/10.5194/egusphere-2025-1700
Preprint. Discussion started: 9 May 2025

Jaramillo. 2020a. 'Air Pollution in Kigali, Rwanda: Spatial and Temporal Variability, Source Contributions, and the Impact of Car-Free Sundays'. *Clean Air Journal* 30(2):1–15. doi: 10.17159/caj/2020/30/1.8023.

Subramanian, R., Abdou Safari Kagabo, Valerien Baharane, Sandrine Guhirwa, Claver Sindayigaya, Carl Malings, Nathan J. Williams, Egide Kalisa, Haofan Li, Peter Adams, Allen L. Robinson, H. Langley DeWitt, Jimmy Gasore, and Paulina Jaramillo. 2020b. 'Air Pollution in Kigali, Rwanda: Spatial and Temporal Variability, Source Contributions, and the Impact of Car-Free Sundays'. *Clean Air Journal* 30(2):1–15. doi: 10.17159/caj/2020/30/1.8023.

Taghian, Gabriella, Samantha Fisher, Thomas C. Chiles, Agnes Binagwaho, and Philip J. Landrigan. 2024. 'The Burden of Cardiovascular Disease from Air Pollution in Rwanda'. *Annals of Global Health* 90(1). doi: 10.5334/aogh.4322.

Teledyne. 2016. *Model T640 PM Mass Monitor*.

UN Environment. 2018. *Kigali City Air Quality Policy and Regulatory Situational Analysis A Report Published by UN Environment in Collaboration with Environmental Compliance Institute*.

UN Environment, REMA. 2019. *Kigali City Air Quality Policy and Regulatory Situational Analysis A Report Published by UN Environment in Collaboration with Environmental Compliance Institute*.

WaveMetrics, Inc. ,. Oregon USA. 2024. 'Igor pro Wave Matrix(Last Accessed: Nov 2024)'. *Https://Www.Wavemetrics.Com/Downloads/Current/Igor%20Pro%209*.

Werden, Benjamin S., Michael R. Giordano, Khadak Mahata, Md Robiul Islam, J. Douglas Goetz, Siva Praveen Puppala, Eri Saikawa, Arnico K. Panday, Robert J. Yokelson, Elizabeth A. Stone, and Peter F. DeCarlo. 2023. 'Submicron Aerosol Composition and Source Contribution across the Kathmandu Valley, Nepal, in Winter'. *ACS Earth and Space Chemistry* 7(1):49–68. doi: 10.1021/acsearthspacechem.2c00226.

West, Sarah E., Patrick Büker, Mike Ashmore, George Njoroge, Natalie Welden, Cassilde Muhoza, Philip Osano, Jack Makau, Patrick Njoroge, and William Apondo. 2020. 'Particulate Matter Pollution in an Informal Settlement in Nairobi: Using Citizen Science to Make the Invisible Visible'. *Applied Geography* 114. doi: 10.1016/j.apgeog.2019.102133.

WHO. 2025. 'Air Pollution Data Portal(Last Accessed: Feb 2025)'. *Https://Www.Who.Int/Data/Gho/Data/Themes/Air-Pollution*.

WHO. n.d. 'Ambient (Outdoor) Air Pollution(Last Accessed: Dec 2024)'. *Https://Www.Who.Int/News-Room/Fact-Sheets/Detail/Ambient-(Outdoor)-Air-Quality-and-Health*. Retrieved 22 April 2025 (https://www.who.int/news-room/fact-sheets/detail/ambient-(outdoor)-air-quality-and-health).

World bank. 2021. *Rwanda Climate Risk Country Profile*.

Zhang, Qi, Jose L. Jimenez, Manjula R. Canagaratna, Ingrid M. Ulbrich, Nga L. Ng, Douglas R. Worsnop, and Yele Sun. 2011. 'Understanding Atmospheric Organic Aerosols via Factor Analysis of Aerosol Mass Spectrometry: A Review'. *Analytical and Bioanalytical Chemistry* 401(10):3045–67.